University of Tehran Press

DESERT

Online Issn: 475-2345X

Home page: https://jdesert.ut.ac.ir/

Estimation of actual evapotranspiration using SEBAL and METRIC algorithms and validation with lysimetric data in arid regions

Vahid Davarzani[1], Mehdi Vafakhah[1]✉, Hamidreza Moradi[1]

1- Department of Watershed Management Engineering, Faculty of Natural Resources, Tarbiat Modares University, Noor, Iran, Email: vafakhah@modares.ac.ir,

Article Info

Article type:
Research Article

Article history:

Received 7 February 2022

Received in revised form 5 April 2022

Accepted 7 September 2022

Published online 25 September 2022

Keywords:
Actual evapotranspiration,
Energy balance algorithm,
Remote sensing,
Water management

ABSTRACT

Estimation of actual evapotranspiration (ET) in large areas is an important part of water resources management. In recent years, remote sensing has been successfully used in ET estimation, which is supposed to be more accurate for estimating ET on regional and agricultural scales. The main aim of this investigation is to evaluate the efficiency of two algorithms namely Surface Energy Balance Algorithms for Land (SEBAL) and Mapping ET at high Resolution with Internalized Calibration (METRIC) algorithms for estimating actual ET from agricultural lands in Davarsen County, Iran. Accordingly, six Landsat 8 OLI/TIR satellite images and Lysimeter data installed in these lands were used. The amounts of actual ET were estimated using two algorithms and the obtained results were compared with Lysimeter data. Based on the results of evaluation, Root Mean Square Error (RMSE) of 0.54 and 0.64 mm day^{-1}, Nash-Sutcliffe Efficiency (NSE) criteria of 0.85 and 0.79, Mean Bias Error (MBE) of 0.04 and 0.02 mm day^{-1}, Mean Absolute Error (MAE) of 0.42 and 0.48 mm day^{-1} and coefficient of determination (R^2) of 0.86 and 0.82 were estimated for SEBAL and METRIC algorithms, respectively. These statistical indices show that these algorithms have a high accuracy for estimating actual ET in the study area. The executive applications of this study can be used to determine the exact amount of evapotranspiration in irrigated lands for water allocation planning, optimization of crop production, irrigation management and assessment of land use change on water efficiency.

Cite this article: V. Davarzani, M. Vafakhah & Moradi HR. (2022). Estimation of actual evapotranspiration using SEBAL and METRIC algorithms and validation with lysimetric data in arid regions. DESERT, 27 (2), DOI: 10.22059/jdesert.2022.90828

 Publisher: University of Tehran Press.
DOI: 10.22059/jdesert.2022.90828

Introduction

Water is often the most limiting factor for agriculture development in arid and semi-arid areas. Overload use from water and recent droughts has been caused great difficulties in water resources. Variety and plurality of water resource and various water uses in different and various sectors cause present age to be meet water deficit difficulty (Yang and Shang, 2013). In order to exit from water crisis, water resource management is necessary (Babrian and Honarbakhsh, 2008). Water resource management as a necessity solution, need more acknowledgment and knowing more understanding of complicated collection from interactions related to water balance components (Modiri and Modiri, 2016). Determination of water balance components is an effective method in water resource management. Whereas evapotranspiration (ET) process is one of the important components in hydrological cycle, this

process should be analyzed in various temporal and spatial scales (Abrishamkar and Ahmadi, 2017). During ET process, water is lost on the one hand from the soil surface by evaporation and other hand from the crop by transpiration. Using of satellite data due to the limited number of climatological stations and costly data collection have some advantages compared with ground-based observation of ET. In addition, satellite data can be used in regional-scale studies (Bastiaanssen *et al.*, 2005).

Satellite data are applied for deriving ET using energy balance techniques. Surface Energy Balance Algorithms for Land (SEBAL) and Mapping ET at high Resolution with Internalized Calibration (METRIC) were presented by Bastiaanssen (1998a,b) and Allen et al. (2007), respectively. SEBAL has been applied and validated in different parts of the world (Diak, 1993; Bastiaanssen *et al.*, 1998b; Bastiaanssen, 2000; Hafeez and Chemin, 2002; Allen *et al.*, 2003; Bastiaanssen *et al.*, 2005; Kimura *et al.*, 2007; Zwart and Bastiaanssen, 2007; Li *et al.*, 2008; Teixeira *et al.*, 2009; Yang *et al.*, 2012; Tang *et al.*, 2013; Sari *et al.*, 2013; Zhou *et al.*, 2014; Bhattarai *et al.*, 2017; Wagle *et al.*, 2017; Spiliotopoulos *et al.*, 2017; Filgueiras *et al.*, 2019; Wolff *et al.*, 2022). METRIC has been validated by Folhes *et al.* (2009) and Filgueiras *et al.*, (2019) in Brazil, Carmona *et al.* (2017) in Argentina, Wagle *et al.* (2017) in USA, Spiliotopoulos *et al. (*2017) in Ireland and Jaafar and Ahmad (2020) in Lebanon.

Several attempts have been made to validate SEBAL and METRIC using Lysimeter data. Tasumi *et al.* (2003, 2005) validated SEBAL and METRIC using Lysimeter in two regions of southern Idaho, USA. The validation results showed that both SEBAL and METRIC can estimate ET accurately in agricultural land use. Allen *et al.* (2003) compared SEBAL with Lysimeter data in USA. The difference between monthly and seasonal ET by SEBAL and Lysimeter data were 16% and 4.3%, respectively. Paul *et al.* (2013) applied SEBAL on 10 high-resolution airborne images acquired during Bushland Evapotranspiration and Agricultural Remote Sensing Experiment 2008 (BEAREX08) and validated using four large weighing Lysimeter installed on two irrigated and two dryland fields in Texas, USA. The validation results showed that instantaneous ET can estimate accurately with mean bias error (MBE) and root mean square error (RMSE) of 0.13 and 0.15 mm h^{-1} (23.8 and 28.2%) respectively. So far SEBAL and METRIC have only been applied with Landsat 5 (TM) and Landsat 7 (ETM^{+}) images and validated using Lysimeter data (Tasumi *et al.*, 2003, 2005; Allen *et al.*, 2003, 2005). Thus, SEBAL and METRIC have been applied with Landsat 8 OLI/TIRS and validated using one drainage Lysimeter installed on irrigated wheat fields during the 2017 growing season in Sabzevar County plain, Iran.

Material and methods

Study area

The Sabzevr County plain with 57 km^2 in area is located between 50˚67′ and 53˚46′ E longitudes, and 40˚02′ and 40˚09′ N latitudes in Khorasan Razavi Province, the eastern part of the Iran (Fig. 1). The mean of elevation, temperatures and precipitation are 977m above sea level, 18.6˚C and 150.7mm, respectively. The climate of the study area is arid based on climate classification system of Domarton (Hoseinalizadeh *et al.*, 2006).

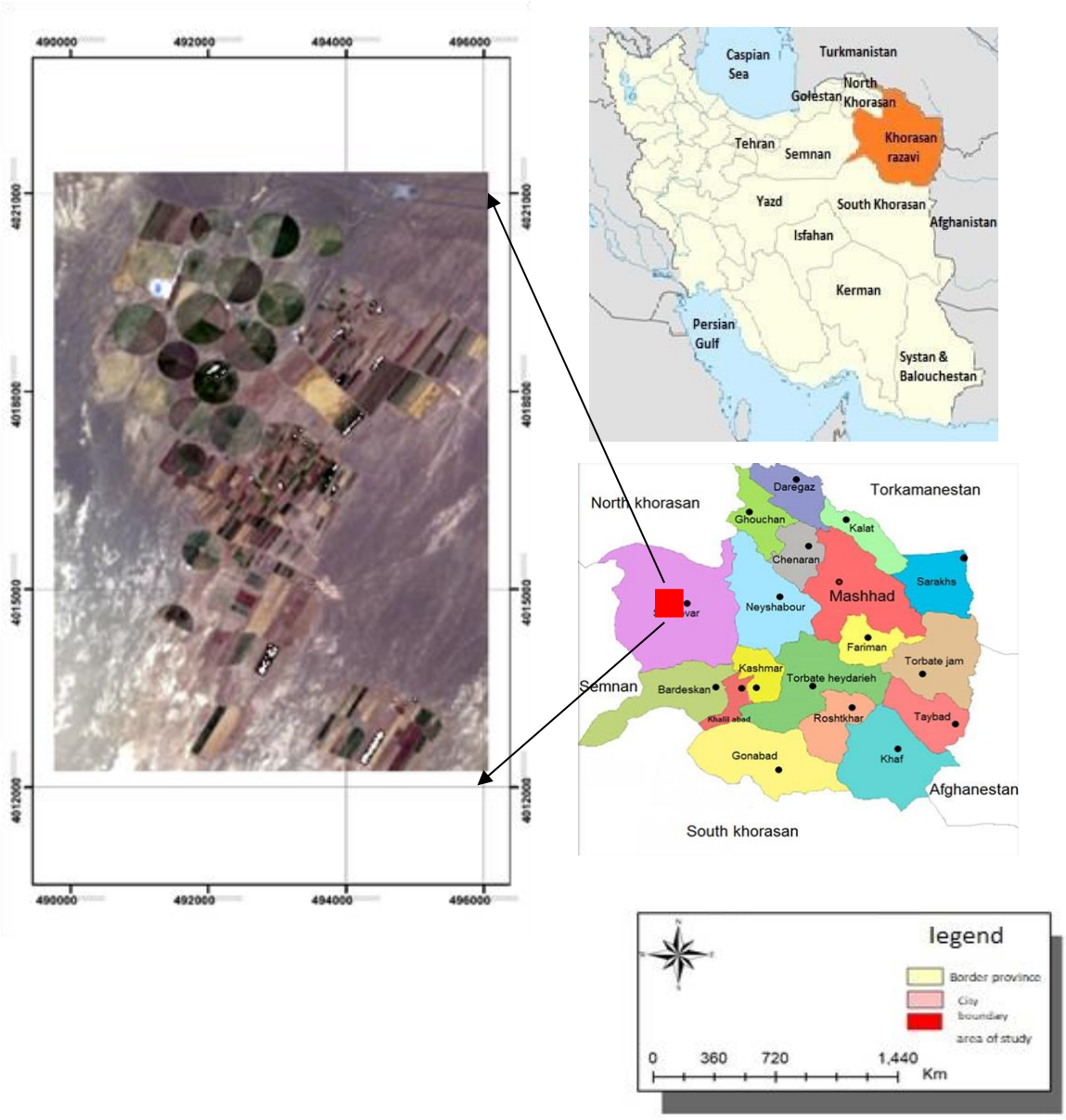

Figure 1. Location of the study area in Razavi Khorasan Province, Iran

Landsat images

The SEBAL and METRIC models were implemented on six images of Landsat 8 OLI/TIR Level 2 obtained from the US Geological Survey (USGS) archive (http://earthexplorer.usgs.gov/) covering Sabzevar County plain (Table 1).

Table 1. Landsat 8 OLI/TIRS satellite imageries used for ET comparison and application

Path/row	Date	Overpass time (local)
161/35	02/26/2017	10:19:39 a.m.
161/35	03/14/2017	10:19:26 a.m.
161/35	03/30/2017	10:19:09 a.m.
161/35	04/15/2017	10:19:10 a.m.
161/35	05/01/2017	10:19:07 a.m.

161/35 05/17/2017 10:19:06 a.m.

Landsat-8 Level 2 products are surface reflectance products. These products have been provided in the georeferenced form. Geometric, atmospheric and radiometric corrections have been carried out on these products.

Measurement ET

A percolation (drainage) Lysimeter (1×1m in area and 1.2 m in depth) was set up in irrigated wheat fields with 180 ha in area to continuously measure actual ET within three months in the 2017 growing season (Fig. 2) (Howell 2005). To set up Lysimeter in farmland, a hole was dug greater than the one dimension. It was installed so that all the edge and part of Lysimeter the same as farmland level. It was filled with 20 cm gravel and sand layer Lysimeter bottom. We also measured daily soil moisture (TDR, Delta TML3) in different depths within three months.

Figure 2. The drainage Lysimeter (right photo) used in this study

SEBAL and METRIC models

A brief overview to SEBAL and METRIC models present as follow, further theoretical details available in Allen *et al.* (2007). In these models, actual ET are calculated using satellite images based on energy balance. Since the satellite image only provides information about the overpass time, the SEBAL and METRIC models compute instantaneous ET flux in the time image (Folhes *et al.*, 2009). The ET flux for each pixel of image is calculated as:

$$\lambda ET = R_n - H - G \quad (1)$$

where λET is latent heat flux (Wm^{-2}) which is easily converted to actual ET, R_n is net radiation (Wm^{-2}), H is sensible heat flux (Wm^{-2}) and G is soil heat flux (Wm^{-2}).

Net radiation (R_n) is calculated from balance between incoming and outgoing radiation fluxes as:

$$R_n = (1-\alpha)R_{S\downarrow} + R_{L\downarrow} - R_{L\uparrow} - (1-\varepsilon_0)R_{L\downarrow} \quad (2)$$

where α is surface albedo for short wave radiation;$R_{S\downarrow}$ is incoming short wave radiation (Wm^{-2}); $R_{L\downarrow}$ and $R_{L\uparrow}$ are incoming and outgoing long wave radiation (Wm^{-2}), respectively; and ε_0 is broad-band surface emissivity.

G is computed as a fraction of $R_n$using Bastiaanssen et al. (2000) in SEBAL model as:

$$\frac{G}{R_n} = \frac{T_s}{\alpha}(0.0038\alpha + 0.0074\alpha^2)(1 - 0.98NDVI^4) \quad (3)$$

where T_s is surface temperature (˚C) and $NDVI$ is Normalized Difference Vegetation Index. G is computed using Tasumi (2003) in METRIC model as:

$$\frac{G}{R_n} = 0.05 + 0.18e^{-0.521LAI} \quad LAI \geq 0.5 \quad (4)$$

$$\frac{G}{R_n} = 1.8(T_S - 273.15)/R_n + 0.084 \quad LAI < 0.5 \quad (5)$$

where LAI is Leaf Area Index.

H is the key part of SEBAL and METRIC models which is determined using an interactive process from an aerodynamic function as (Allen et al. 2002):

$$H = \frac{(\rho . C_P . dT)}{r_{ah}} \quad (6)$$

$$u_* = \frac{u_{200}k}{\ln\left(\frac{200}{z_{0m}}\right) - \Psi_{m(200)}} \quad (7)$$

$$r_{ah} = \frac{\ln\left(\frac{z_2}{z_1}\right) - \Psi_{h(z_2)} + \Psi_{h(z_1)}}{u_* \times k} \quad (8)$$

where ρ is the density of air (kgm^{-3}); C_p is the specific heat of air (1004 J kg^{-1}K^{-1}); dT is temperature difference (°K) between two near-surface heights (z_1, z_2); r_{ah} is the aerodynamic resistance (sm^{-1}); $u_{200}$is wind speed at 200m (m s^{-1}); kis Von Karman's constant (0.41);z_{0m} is the roughness length for momentum transfer; z_1 and $z_2$are heights above the zero-plane displacement of the vegetation assumed 0.1 and 2 m, respectively; and Ψ_m and Ψ_h are stability corrections for momentum and heat transport, respectively.

Solving the Equation 6 is difficult because of existence of two unknown parameters (r_{ah} and dT), therefore it is selected two pixels i.e. cold and hot pixels in the study area. The cold pixel was selected within areas covered with well-irrigated wheat fields, which it is assumed surface temperature equal to near surface temperature. At cold pixel, all available energy is used for latent heating in SEBAL model, meanwhile in METRIC model, ET is 5% more than reference ET for alfalfa (Bhattarai *et al.*, 2017). As the same way, the hot pixel was selected within areas without any vegetation which it is assumed ET is 0. In selection of these pixels, some factors such as surface temperature, albedo and vegetation indices were used. In selection of hot/cold pixels, it was considered to avoid very low or very high temperature selection.

After determining H and all the other components in energy balance equation (R_n and G), the instantaneous values of λET were calculated for each pixel of six Landsat images used in the study using Equation 1. The instantaneous value of actual ET is obtained as:

$$ET_{inst} = 3600\frac{\lambda ET}{\lambda \times \rho_{air}} \quad (9)$$

where ET_{inst} is the instantaneous value of actual ET for the image time(mm h^{-1});λ is the latent heat of vaporization(J kg^{-1}); $\rho_{air}$is air density (kg m^{-3}); and 3600 is the time conversion from seconds to hours. The λvalue is obtained using Equation 10 (Allen et al., 2002):

$$\lambda = [2.501 - 0.00236(T_S - 273.15)] \times 10^6 \quad (10)$$

In SEBAL model, evaporative fraction (∧) is computed as a ratio of latent heat to available energy, while in METRIC model,$ET_r.F$is computed as a ratio of instantaneous ET for each pixel

to the reference ET obtained from meteorological data using FAO-Penman-Montieth version 56:

$$ET_rF = \frac{ET_{inst}}{ET_r} \quad (11)$$

Finally, by assuming that ∧ and ET_rF are constant for each day, daily actual ET (ET_{24}) are computed as:

$$ET_{24}(\text{SEBAL}) = \frac{ET_{inst} \times R_{n24}}{G - R_n} \quad (12)$$

$$ET_{24}(\text{METRIC}) = ET_rF \times ET_{r\_24} \quad (13)$$

Daily actual ET depends on R_n, wind velocity and air temperature during the satellite overpass time. The wind velocity and air temperature during the satellite overpass time are given in Table 2.

Table 2. The values of air temperature and wind velocity in the six days of the studied image

Date	02/26/2017	03/14/2017	03/30/2017	04/15/2017	05/01/2017	05/17/2017
Air temperature (°C)	11	13.1	15.2	16.5	17.2	18
Wind velocity(m s^{-1})	4	6.3	3.4	5.1	7.8	9.3

Models Assessment

Hourly and 24 hours values of actual ET obtained Lysimeter were used to validate SEBAL and METRIC models. Root Means Square Error (RMSE), Mean Bias Error (MBE), Mean Absolute Error (MAE), Nash-Sutcliff Efficiency (NSE) coefficient and coefficient of determination (R^2) were used for statistical assessment of the models accuracy.

Results

Energy balance maps

As shown in Fig. 3, NDVI varies between -1 and 1 and LAI varies between 0 and 5.7. The values of NDVI and LAI show crop growth in the studied farmland area. Actually, comparing the values of NDVI and LAI and their distribution variability in the study area show that where NDVI is high, LAI is also high. On the other words, NDVI and LAI correspond to each other. Comparing the NDVI (Fig. 3), surface temperature (Fig. 4) and actual ET (Figs. 9 and 10) maps indicate that in the areas where NDVI is high and the surface temperature is low, the actual ET will be more.

The farmland areas with high NDVI and LAI shows relatively low albedo and surface temperature and relatively high net radiation. The result shows that the greater part of available energy in these areas are used for ET process and decreasing temperature occurs. For example, NDVI, surface temperature, surface albedo and maps are given in Figs. 3-5. Comparison of Fig. 4 with Figs. 9 and 10 also confirm this matter.

The low value of soil heat flux in the study area given in Fig. 6 is probably due to wet surface soil by irrigation or local rainfall. As shown in Figs. 4 and 6, in areas where soil heat flux is low, the surface temperature is also low. Accordingly, the higher surface temperature, the higher soil heat flux and vice versa.

As can be seen from the data in Table 2, wind velocity is the most at 17 May 2017 that it is reasonable due to season and climate in the study area but air temperature from the first image (26 February 2017) to the sixth image (17 May 2017) has increasing trend. It is apparent from Tables 2 and 4 and Figs. 4, 9 and 10 that the actual ET accords with the air temperature and surface temperature values.

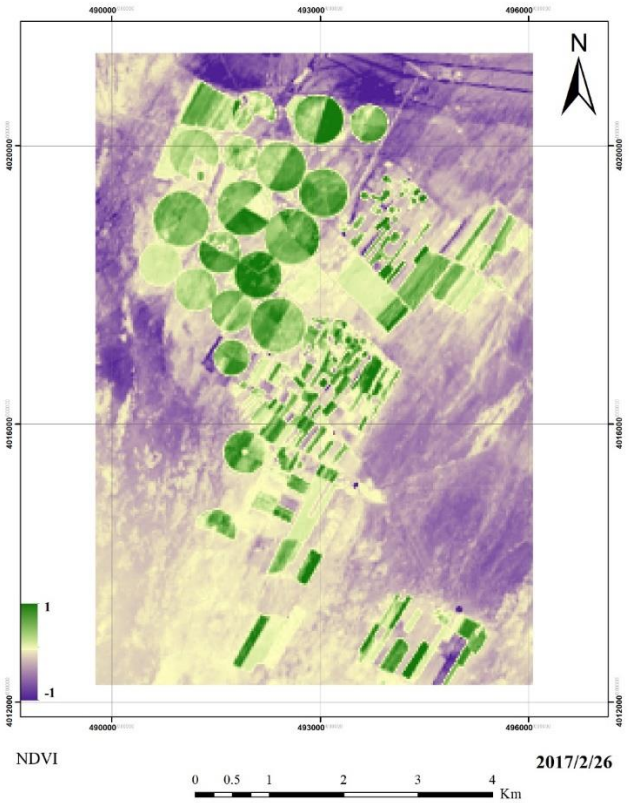

Figure 3. Normalized difference vegetation index (NDVI)

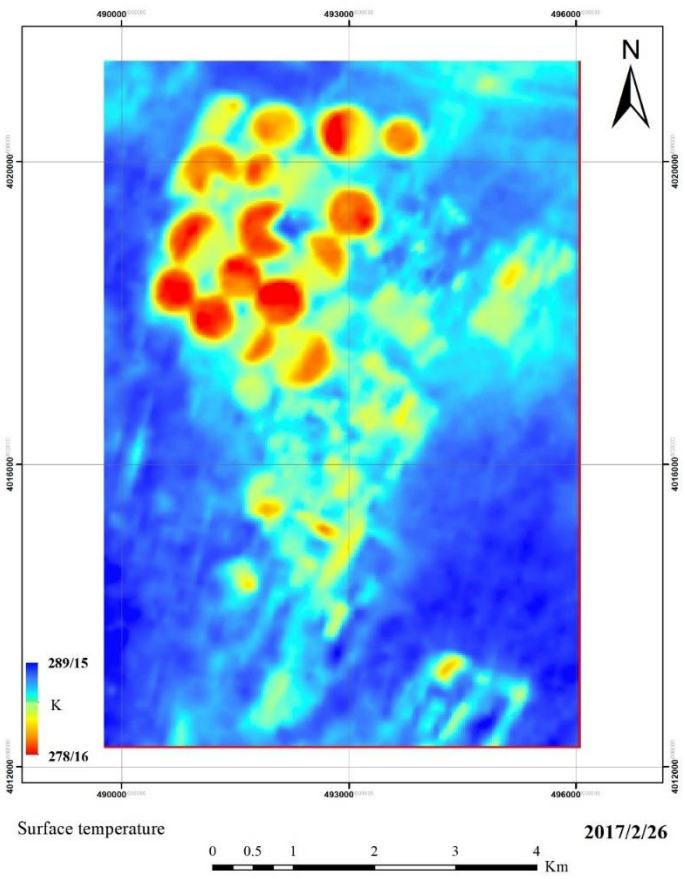

Figure 4. Surface temperature (T, ˚K)

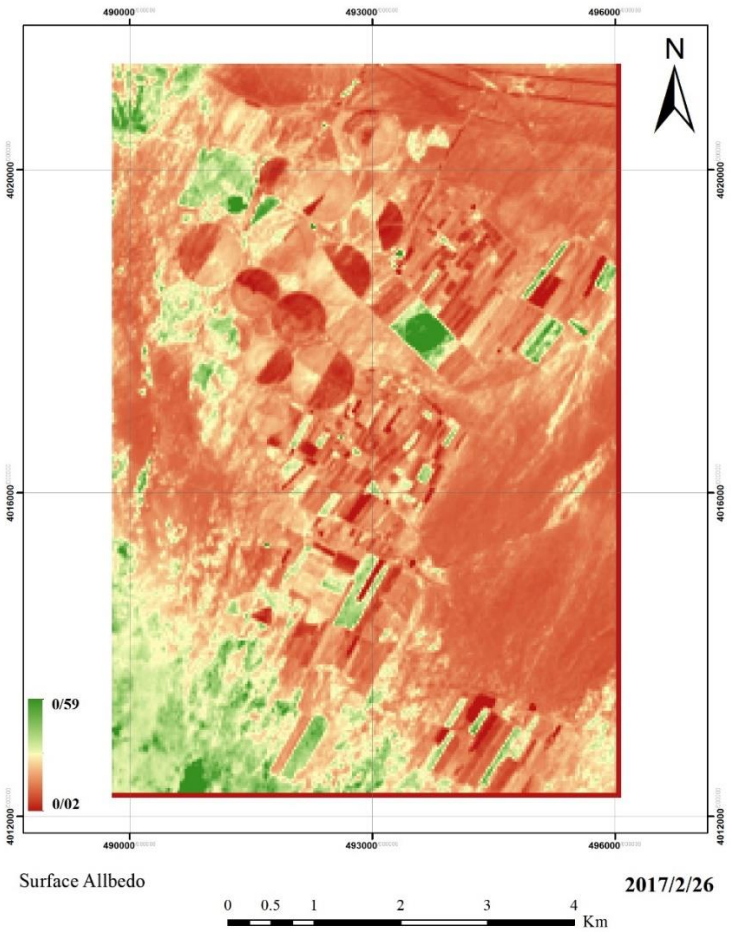

Figure 5. Surface albedo (α)

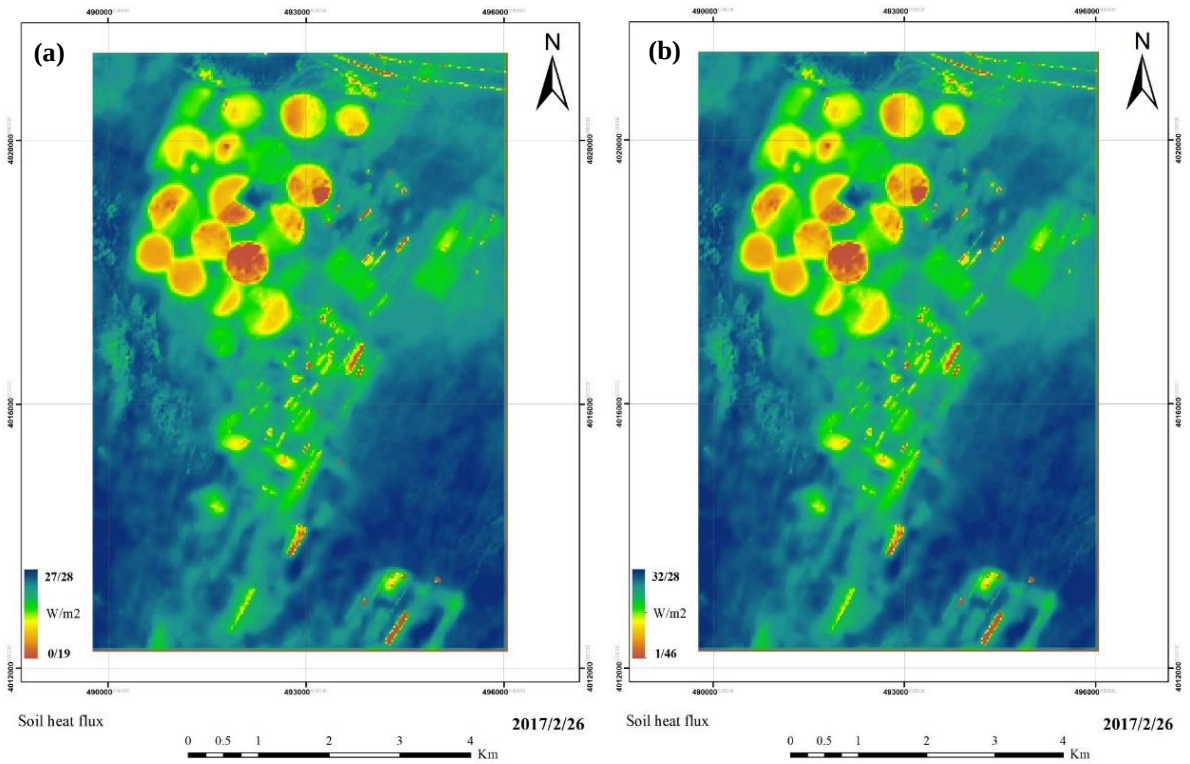

Figure 6. Soil heat flux (G, W m^{-2}) (a) SEBAL, (b)METRIC

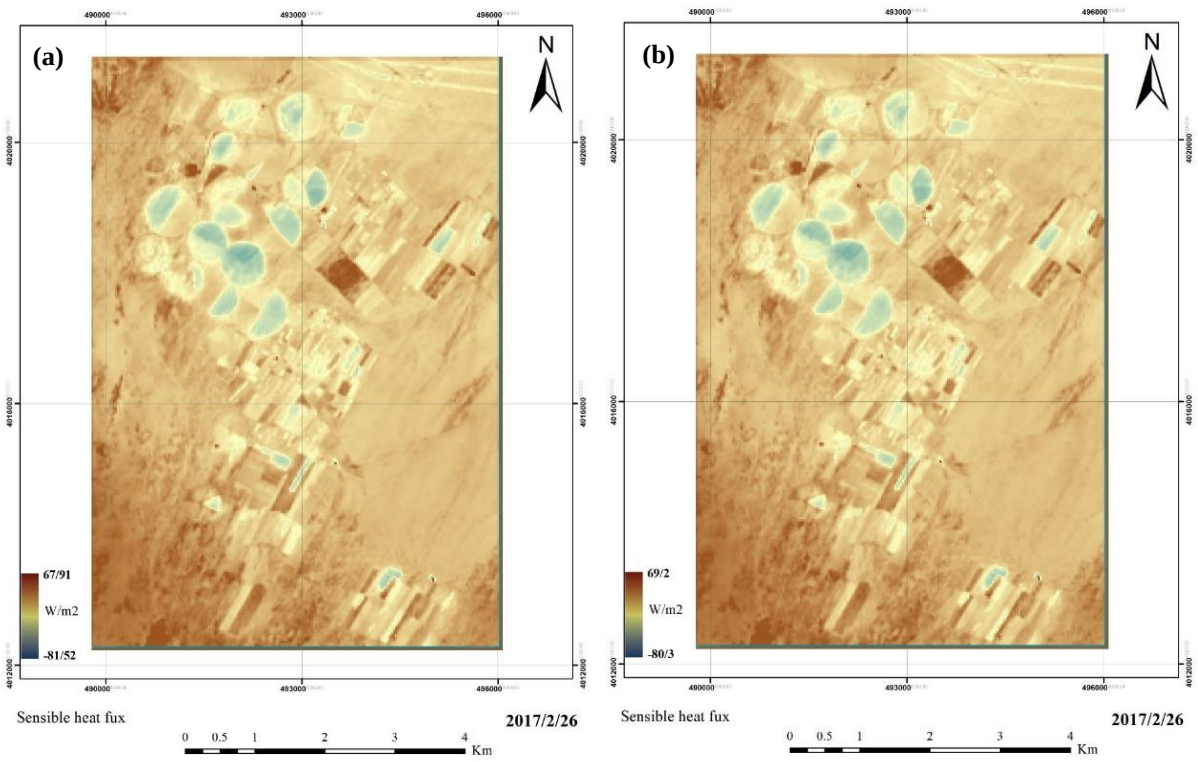

Figure 7. Sensible heat flux (H, W m^{-2}) (a) SEBAL, (b)METRIC

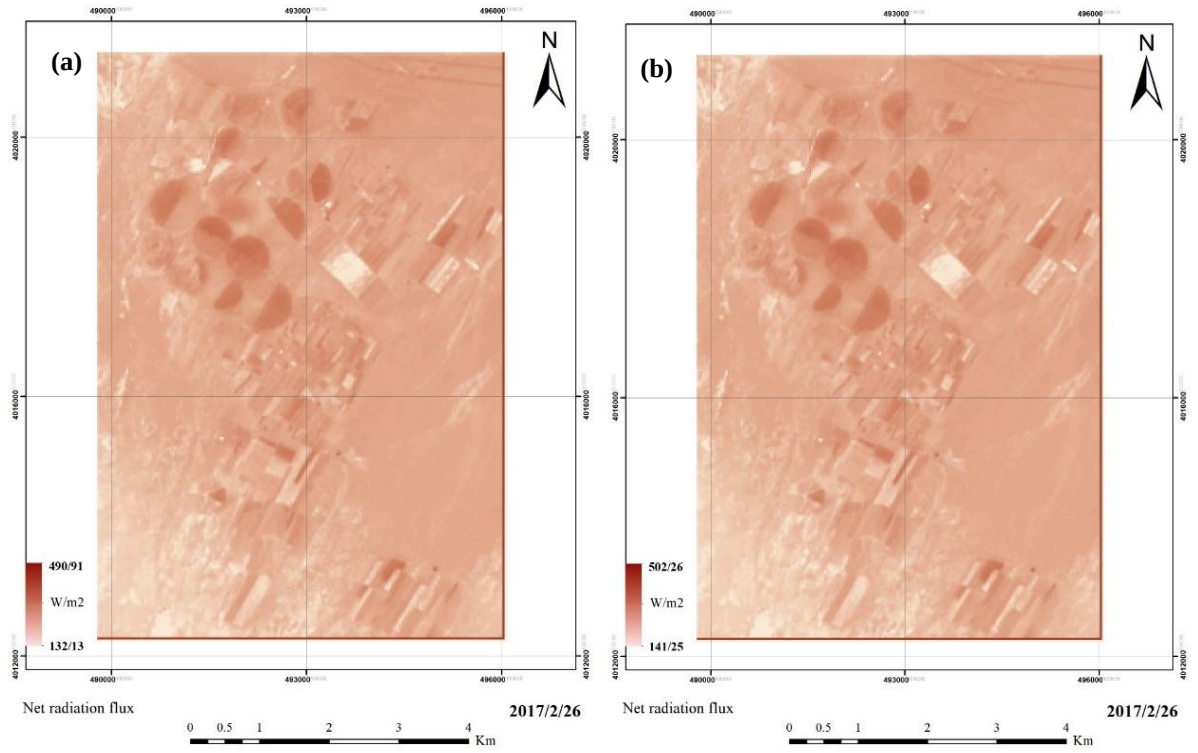

Figure 8. Net Radiation flux (Rn, W m^{-2}) (a) SEBAL, (b)METRIC

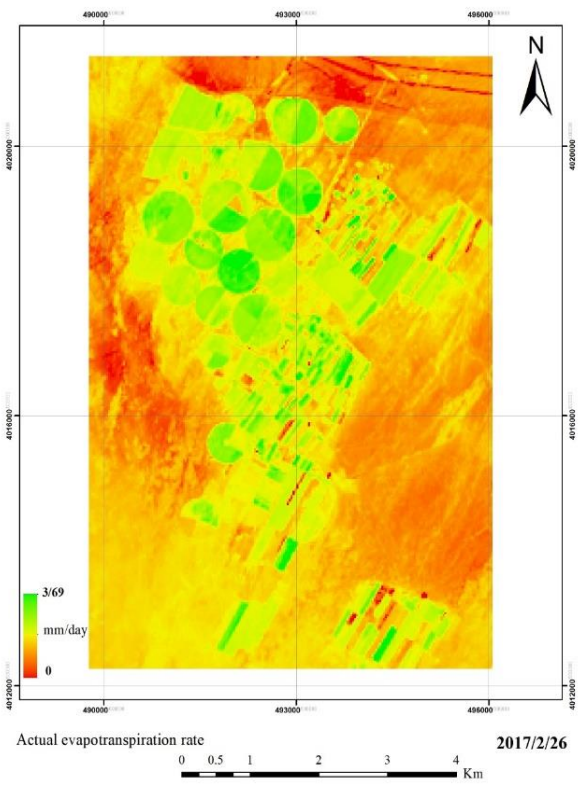
N
3/69
mm/day
0
Actual evapotranspiration rate
2017/2/26
0 0.5 1 2 3 4
Km

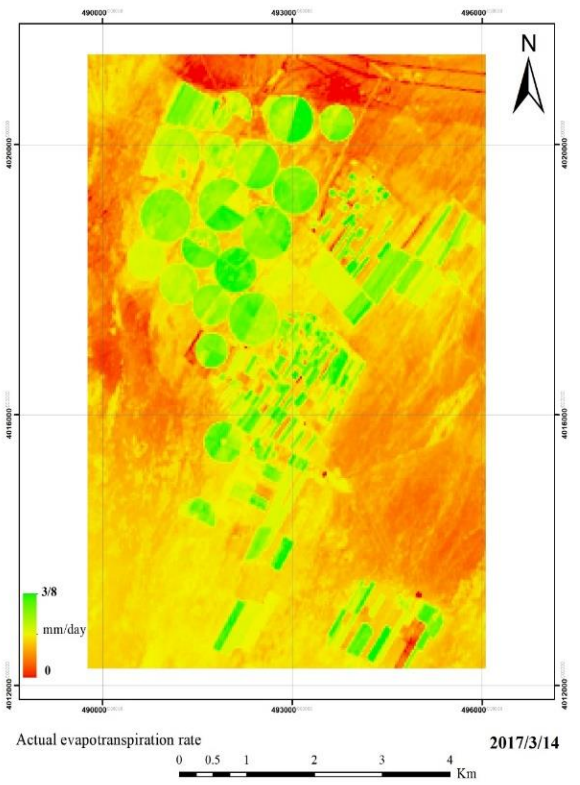
N
3/8
mm/day
0
Actual evapotranspiration rate
2017/3/14
0 0.5 1 2 3 4
Km

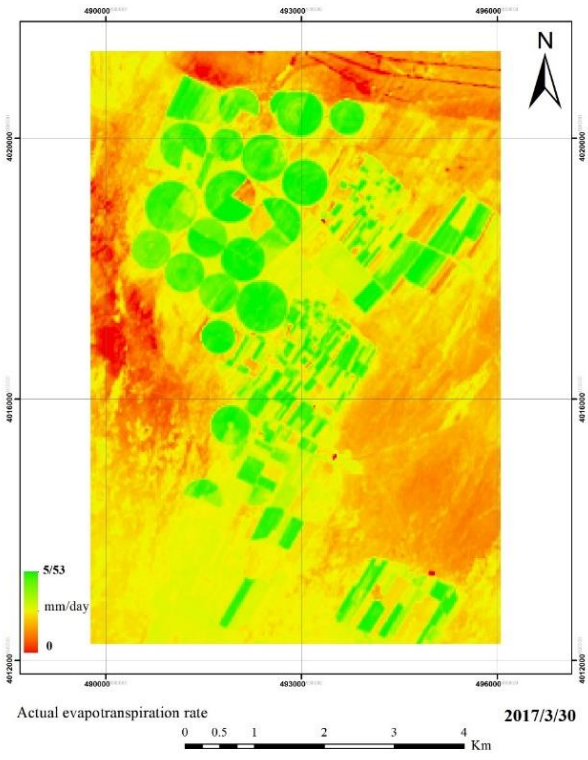
N
5/53
mm/day
0
Actual evapotranspiration rate
2017/3/30
0 0.5 1 2 3 4
Km

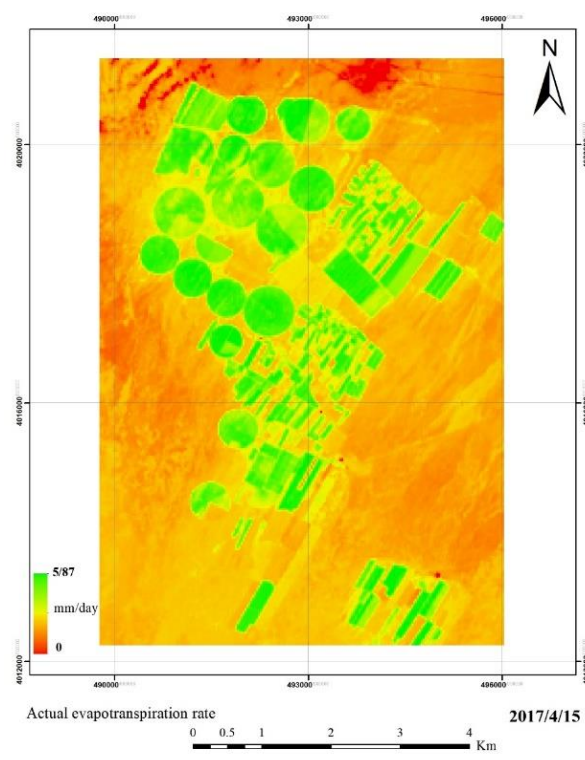
N
5/87
mm/day
0
Actual evapotranspiration rate
2017/4/15
0 0.5 1 2 3 4
Km

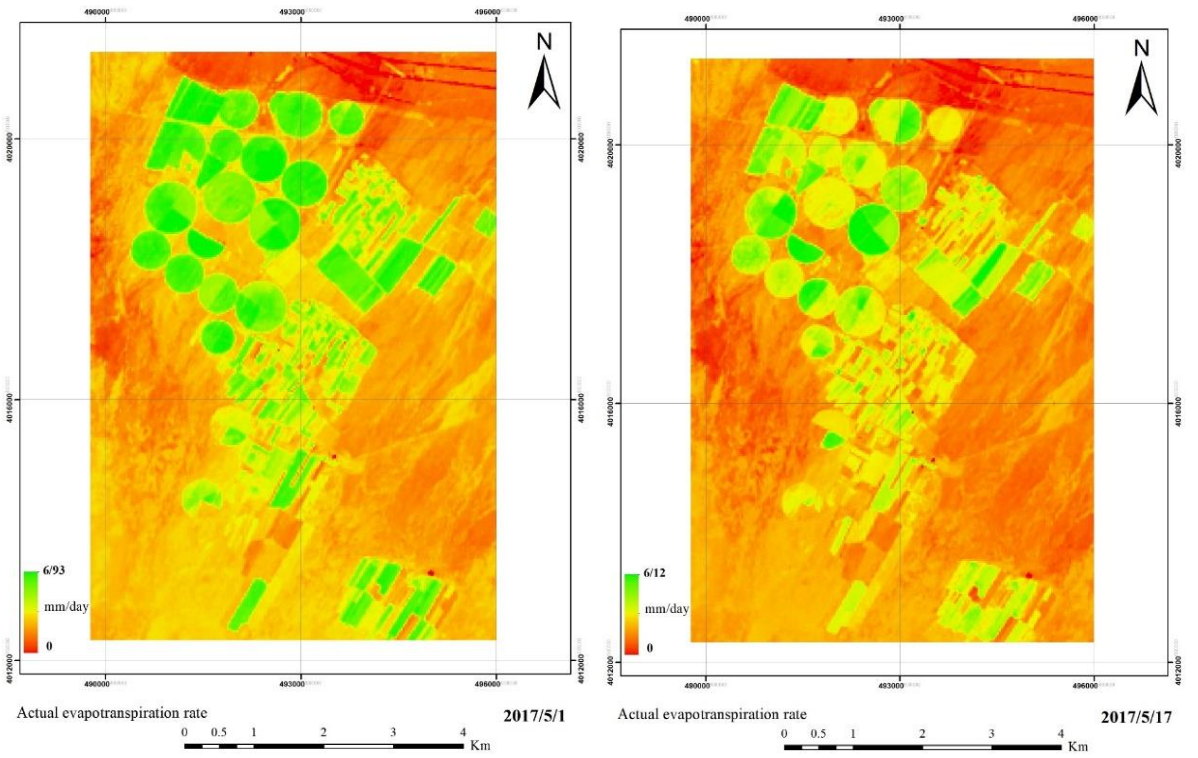

Figure 9**. Daily actual ET (mm day^{-1}) by SEBAL**

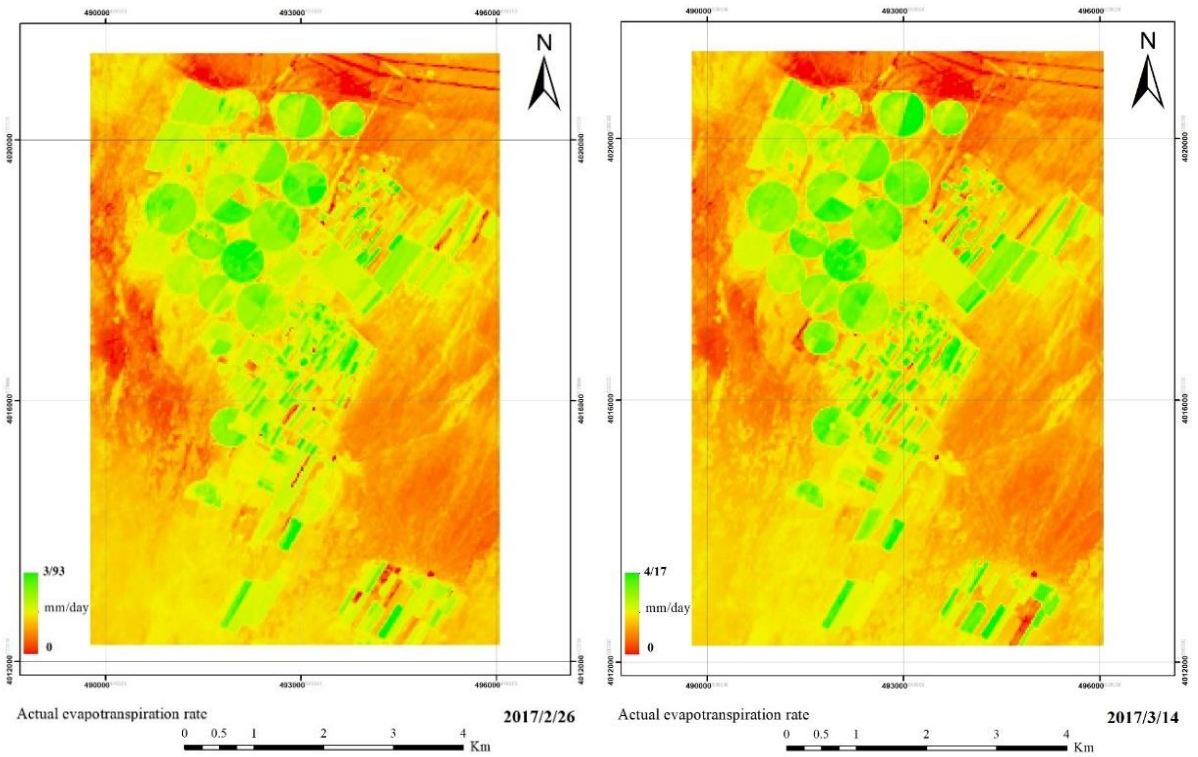

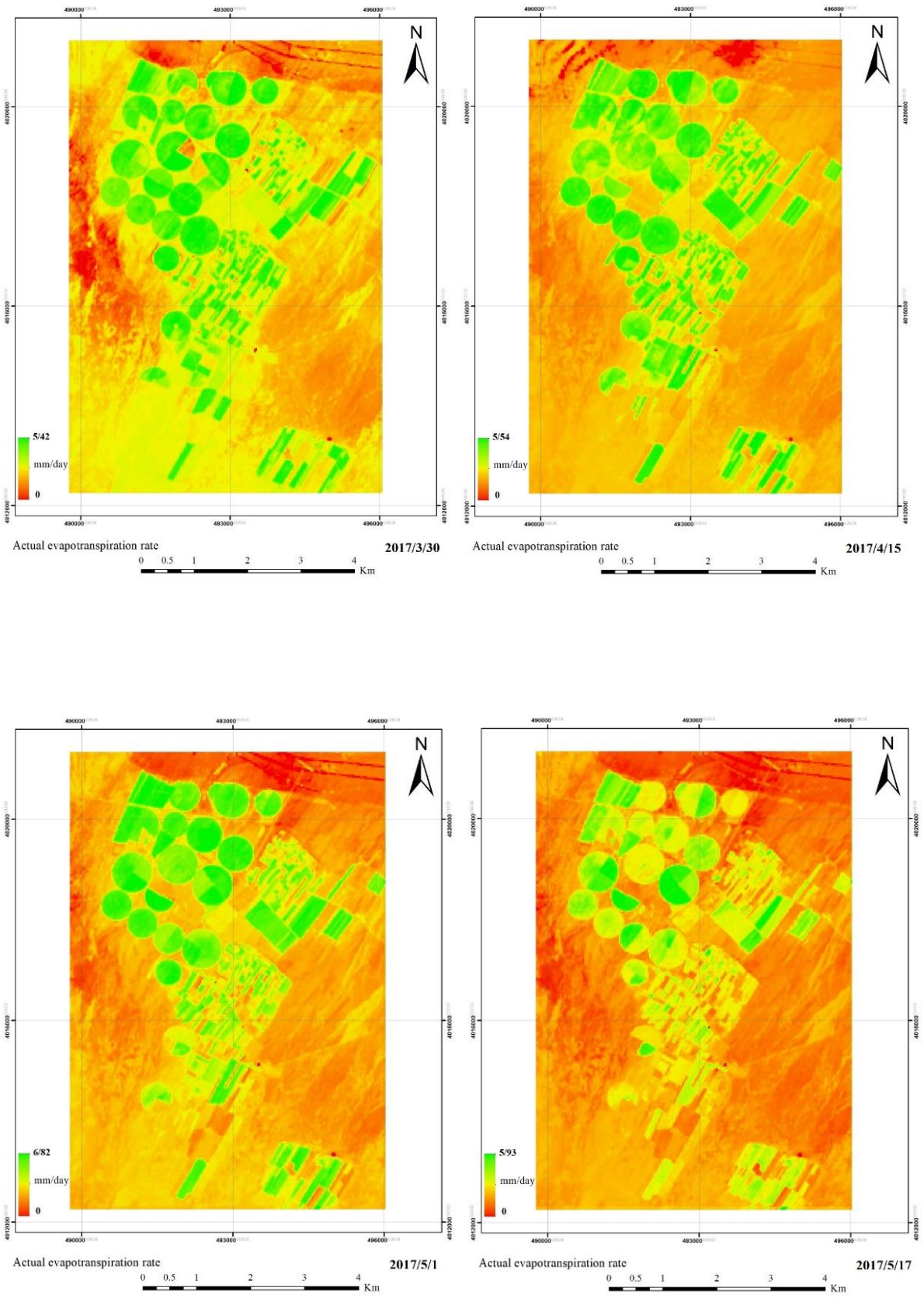

Figure 10. Daily actual ET (mm day^{-1}) by METRIC

Selection of hot and cold pixels

Surface temperature, NDVI and albedo were considered for selecting the hot and cold pixels in the study area. In this method, the desert was removed using the land use map. Then, filters were applied based on the NDVI, albedo, and surface temperature images to identify potential candidate pixels for hot and cold pixels. In the end, the best-conditioned pixel was selected. The cold pixel has low surface temperature, high NDVI and low albedo (0.22-0.24) but the hot pixel has high surface temperature, low NDVI (0-0.4) and high albedo. The pixels with maximum surface temperature were not selected as the hot pixel in the study area because desert areas have usually higher temperature than the barren farmland areas. Accordingly, if the hot pixel selected in these area, ET would be positive in the barren areas with lower temperature. Table 3 shows characteristics of hot and cold pixels.

Table 3. Selection of cold and hot pixel

Date		Albedo	NDVI	LAI	T(˚K)
02/26/2017	Cold pixel	0.231	0.662	2.394	281.231
	Hot pixel	0.159	0.009	0	287.173
03/14/2017	Cold pixel	0.224	0.752	1.949	293.973
	Hot pixel	0.252	0.121	0.021	297.325
03/30/2017	Cold pixel	0.231	0.935	2.611	296.695
	Hot pixel	0.169	0.003	0	302.937
04/15/2017	Cold pixel	0.229	0.871	2.243	299.782
	Hot pixel	0.148	0.064	0	306.283
05/01/2017	Cold pixel	0.241	0.731	2.435	311.324
	Hot pixel	0.313	0.025	0	317.621
05/17/2017	Cold pixel	0.237	0.882	2.163	313.231
	Hot pixel	0.171	0.228	0	320.226

Result from comparison of SEBAL and METRIC models with Lysimeter data

Daily actual ET were computed by SEBAL and METRIC models in the study area (Table 4).

Table 4. The actual ET by SEBAl, METRIC and Lysimeter in the six days of the studied image

Date	02/26/2017	03/14/2017	03/30/2017	04/15/2017	05/01/2017	05/17/2017
ET_{SEBAL}(mm day^{-1})	3.69	3.8	5.53	5.87	6.93	6.12
ET_{METRIC}(mm day^{-1})	3.93	4.17	5.42	5.54	6.82	5.93
$ET_{Lysimeter}$(mm day^{-1})	3.38	3.71	5.31	5.62	6.44	7.25

Table 5 shows five statistical criteria for estimating daily actual ET by SEBAL and METRIC.

Table 5. Performance statistics of SEBAL and METRIC models for daily ET (mm day^{-1}) estimation

Model	n	R^2	RMSE	NSE	MBE	MAE
SEBAL	6	0.86	0.54	0.85	0.04	0.42
METRIC	6	0.82	0.64	0.79	0.02	0.48

Discussion

There is very high correlation between Rn estimation by SEBAL and METRIC and probably little difference is due to τ_{sw} estimation. In SEBAL, τ_{sw} is computed as follows:

$$\tau_{sw} = 0.75 + 2 \times 10^{-5} \times Z \quad (14)$$

where: Z is meteorological station height.

The results obtained from Fig. 8 shows that Rn value obtained by METRIC is slightly higher than of those SEBAL. This result has not previously been described in some published studies (Tasumi *et al.*, 2005; Mutiga, 2014). Of course, the results obtained from the calculated Rn value are only related to six images over a period of almost three months and cannot be generalized over all months and seasons in the study area. The τ_{sw} value according to equation in SEBAL is constant for all months, because it depends only on the meteorological station height.

Because NDVI, LAI, surface albedo and surface temperature are used to calculate the soil heat flux (G) and these parameters are very influential, effect of these parameters on soil heat flux (G) are addressed. Soil heat flux (G) computed by SEBAL and METRIC show the most inconsistency in high surface temperature. Soil heat flux (G) computed by SEBAL is overestimation. This finding is in agreement with French et al.'s (2016) findings. This finding shows that the method used to calculate soil heat flux (G) needs to be verified on the basis of study area characteristics. On the other hand, in order to obtain better result, surface temperature values in the study area should also be investigated (Jia *et al.*, 2016).

Results obtained showed that in the areas where vegetation canopy cover is more due to more ET, the surface temperature is lower and vice versa (Fig. 4). As can be seen from the data in Table 4, daily actual ET value obtained by SEBAL is slightly lower than of those METRIC in farmland areas. In general, energy balance algorithms have been made for farmland areas with vegetation (Bastiaanssen et al., 1998; Allen et al., 2002).

As can be seen from the Table 5, both algorithms predict actual ET good. If RMSE, MAE and MBE are less and close to zero, model performance will be better. R^2, RMSE, NSE, MAE and MBE values are as 0.86 and 0.82, 0.54 and 0.64, 0.85 and 0.79, 0.42 and 0.48 and 0.04 and 0.02mm day^{-1} for SEBAL and METRIC algorithms, respectively. These values shows that the prediction of both algorithms for farmland area are to be acceptable. This finding is consistent with those of Allen et al. (2005), Evans et al. (2005) and Wagle et al. (2005) findings who found SEBAL and METRIC algorithms with R^2 more than 0.80. These results shows a significant accuracy by both algorithms for estimating actual ET. As shown in Table 5 and Fig. , actual ET value estimated by SEBAL and METRIC about 0.50-1 mm day^{-1} more than the observed data (Lysimeter measurement. This finding is in agreement with Oberg et al.'s (2006) and George et al.'s (2013) findings. On the other hand, SEBAL in high actual ET values showed overestimation but METRIC in low ones. This result can be explained by the estimation of soil heat flux (G) and sensible heat flux (H) in the algorithms. Since soil heat flux (G) and sensible heat flux (H) in SEBAL is overestimation in high air temperature (Allen et al., 2002; Bastiaanssen et al., 1998).

The spatial distribution of actual ET in the study area as which are shown in Figs. 9 and 10 , is due to land us type, vegetation species of agricultural and rangeland and cultivation date. The irrigated farming land with high vegetation canopy cover located in northern part of the study area has high NDVI and actual ET in this part is more than mean actual ET of the study area. This result may explain the strongly and positive correlation between NDVI and actual ET. Whereas the temporal variation of actual ET in the study area is due to air temperature and vegetation canopy cover. As can be seen from Figs 9 and 10, actual ET increases from 26 February 2017 to 17 May 2017. This result may be due to increasing air temperature and vegetation canopy cover. As Table 5 shows, the highest computed actual ET (ET_{SEBAL} and ET_{METRIC}) and Lysimeter data (ETLysimeter) were on 1 May 2017 and 17 May 2017, respectively. This difference can be explained in part by the vegetation climax and moisture existence on 1 May 2017. This finding is in agreement with Bashir et al.'s (2008) finding.

Conclusion

The present study was designed to evaluate SEBAL and METRIC performance for estimating the actual ET in farmland areas located in Davarzan County, Iran. The results of this study show that the areas where NDVI is high, the surface temperature is low and other areas where NDVI is low to show high surface temperature. The actual ET in the areas with high NDVI was more in the study area. Also, soil moisture and Rn compared with other parameters such as wind velocity and water vapor pressure shortage have more effect in surface temperature variations. The barren areas (sandy areas, sandy plain, clay plain) have more surface temperature than other areas. This result may be explained by the fact that the dry soil become quickly warm compared with the humid soil in a sunny day, because the specific heat capacity water is more than soil. Meanwhile since the field capacity of the clay soil is more than sandy soil, surface temperature in surface sandy areas is more than clay plain. NDVI shown land cover is consistent with increasing or decreasing trend of under cultivation in the study area. The results of the actual ET are also consistent with NDVI. As the highest actual ET is related to end spring and the lowest is related to early April i.e., starting cultivation season in the study area. The selection of hot and cold pixel is very important in SEBAL and METRIC algorithms. Therefore, the wrong selection of these pixels strongly affects on the SEBAL and METRIC algorithms computation processes. In general, SEBAL and METRIC have the ability to estimate ET distribution. The estimated ET maps using SEBAL and METRIC are very useful to improve water management and allocation.

References

Abrishamkar M, Ahmadi A. 2017. Evapotranspiration estimation using remote sensing technology based on SEBAL algorithm, Iranian Journal of Science and Technology, Transactions of Civil Engineering, 41; 65-76.

Allen R, Tasumi M, Trezza R, Waters R, Bastiaanssen W. 2002. SEBAL (Surface Energy Balance Algorithms for Land), Advance Training and Users Manual–Idaho Implementation, version, 1; 97.

Allen RG, Morse A, Tasumi M. 2003. Application of SEBAL for western US water rights regulation and planning. In Proc. ICID Int. Workshop on Remote Sensing.

Allen RG, Tasumi M, Trezza R. 2007. Satellite-based energy balance for mapping evapotranspiration with internalized calibration (METRIC)—Model, Journal of Irrigation and Drainage Engineering, 133; 380-394.

Babran S, Honarbakhsh N. 2008. Water Crisis in Iran and World. Rahbord, 16, 193-214.

Bastiaanssen W, Noordman E, Pelgrum H, Davids G, Allen R. 2005. SEBAL for spatially distributed ET under actual management and growing conditions, ASCE Journal of Irrigation and Drainage Engineering, 131; 85-93.

Bastiaanssen WG. 1998a. Remote sensing in water resources management: The state of the art. International Water Management Institute, Colombo, Sri Lanka.

Bastiaanssen WG. 2000. SEBAL-based sensible and latent heat fluxes in the irrigated Gediz Basin, Turkey, Journal of Hydrology, 229; 87-100.

Bastiaanssen WG, Pelgrum H, Wang J, Ma Y, Moreno J, Roerink G, Van der Wal T. 1998. A remote sensing surface energy balance algorithm for land (SEBAL).: Part 2: Validation, Journal of Hydrology, 212; 213-229.

Bhattarai N, Quackenbush LJ, Im J, Shaw SB. 2017. A new optimized algorithm for automating endmember pixel selection in the SEBAL and METRIC models, Remote Sensing of Environment,196;178-192.

Carmona F, Rivas R, Kruse E. 2017. Estimating daily net radiation in the FAO Penman–Monteith method, Theoretical and Applied Climatology, 129; 89-95.

Diak GR, Whipple MS. 1993. Improvements to models and methods for evaluating the land-surface energy balance and 'effective'roughness using radiosonde reports and satellite-measured 'skin'temperature data, Agricultural and Forest Meteorology, 63; 189-218.

Filgueiras R, Mantovani EC, Althoff D, Ribeiro RB, Venancio LP, dos Santos RA. 2019. Dynamics of actual crop evapotranspiration based in the comparative analysis of SEBAL and METRIC-EEFLUX, Irriga 1(1); 72-80.

Folhes M, Rennó C, Soares J. 2009. Remote sensing for irrigation water management in the semi-arid Northeast of Brazil, Agricultural Water Management, 96; 1398-1408.

French A, Jacob F, Anderson M, Kustas W, Timmermans W, Gieske A, Su Z, Su H, McCabe M, Li F. 2005. Surface energy fluxes with the Advanced Spaceborne Thermal Emission and Reflection radiometer (ASTER) at the Iowa 2002 SMACEX site (USA), Remote Sensing of Environment, 99; 55-65.

Hafeez M, Chemin Y. 2002. Evapotranspiration Estimation using TERRA/ASTER sensor: A case study in District 1 of UPRIIS, Central Luzon, Philippines, Canadian Journal of Remote Sensing, 101; 81-95.

Hoseinalizadeh M, Ayoubi S, Shataei S. 2006. Comparison of various interpolation methods on evaluation surface soil properties (Case study: Mehr Sabzevar Watershed), Journal of Agricultural Sciences and Natural Resources, 13; 152-162.

Howell TA. 2005. Lysimetry. In Encyclopedia of Soils in the Environment, ed. D. Hillel, 379-386. Oxford: Elsevier.

Jaafar HH, Ahmad FA. 2020. Time series trends of Landsat-based ET using automated calibration in METRIC and SEBAL: The Bekaa Valley, Lebanon, Remote Sensing of Environment, 238; 111034.

Javadian M, Behrangi A, Gholizadeh M, Tajrishy M. 2019. METRIC and WaPOR estimates of evapotranspiration over the Lake Urmia Basin: comparative analysis and composite assessment, Water, 11; 1647.

Jia Z, Liu S, Xu Z, Chen Y, Zhu M. 2012. Validation of remotely sensed evapotranspiration over the Hai River Basin, China, Journal of Geophysical Research: Atmospheres, 117, 113-125.

Kimura R, Bai L, Fan J, Takayama N, Hinokidani O. 2007. Evapo-transpiration estimation over the river basin of the Loess Plateau of China based on remote sensing, Journal of Arid Environments, 68; 53-65.

Li H, Zheng L, Lei Y, Li C, Liu Z, Zhang S. 2008. Estimation of water consumption and crop water productivity of winter wheat in North China Plain using remote sensing technology, Agricultural Water Management, 95; 1271-1278.

Losgedaragh SZ, Rahimzadegan M. 2018. Evaluation of SEBS, SEBAL, and METRIC models in estimation of the evaporation from the freshwater lakes (Case study: Amirkabir dam, Iran), Journal of Hydrology, 561, 523-531.

Mazidi A, Kooshki S. 2015. Simulation of Rainfall-Runoff Process and Estimate of Flood with HEC-HMSModel in Khorramabad Catchment Area, Geography and Development Iranian Journal, 13; 1-10.

Modiri S, Modiri M. 2016. Calibration of separate window model factors to calculate land surface temperature using MODIS images, European Online Journal of Natural and Social Sciences, 5; 546-558.

Mutiga JK, Su Z, Woldai T. 2010. Using satellite remote sensing to assess evapotranspiration: Case study of the upper Ewaso Ng'iro North Basin, Kenya, International Journal of Applied Earth Observation and Geoinformation, 12; S100-S108.

Paul G, Gowda PH, Prasad PV, Howell TA, Staggenborg SA, Neale CM. 2013. Lysimetric evaluation of SEBAL using high resolution airborne imagery from BEAREX08, Advances in Water Resources, 59; 157-168.

Sari DK, Ismullah I, Sulasdi W, Harto A. 2013. Estimation of water consumption of lowland rice in tropical area based on heterogeneous cropping calendar using remote sensing technology, Procedia Environmental Sciences, 17; 298-307.

Spiliotopoulos M, Holden NM, Loukas A. 2017. Mapping evapotranspiration coefficients in a temperate maritime climate using the metric model and landsat TM, Water, 9; 23.

Tang R, Li ZL, Chen KS, Jia Y, Li C, Sun X. 2013. Spatial-scale effect on the SEBAL model for evapotranspiration estimation using remote sensing data, Agricultural and Forest Meteorology, 174; 28-42.

Tasumi M. 2003. Progress in operational estimation of regional evapotranspiration using satellite imagery. In Ph.D.Dissertation, University of Idaho, 357.

Tasumi M. 2019. Estimating evapotranspiration using METRIC model and Landsat data for better understandings of regional hydrology in the western Urmia Lake Basin, Agricultural Water Management, 226; 105805.

Tasumi M, Trezza R, Allen RG, Wright JL. 2003. US Validation tests on the SEBAL model for evapotranspiration via satellite, In 2003 ICID Workshop on Remote Sensing of ET for Large Regions.

Tasumi M, Trezza R, Allen RG, Wright JL. 2005. Operational aspects of satellite-based energy balance models for irrigated crops in the semi-arid US, Irrigation and Drainage Systems, 19; 355-376.

Teixeira AdC, Bastiaanssen WG, Ahmad M.-u.-D, Bos M. 2009. Reviewing SEBAL input parameters for assessing evapotranspiration and water productivity for the Low-Middle Sao Francisco River basin, Brazil: Part A: Calibration and validation, Agricultural and Forest Meteorology, 149; 462-476.

Wagle P, Bhattarai N, Gowda PH, Kakani VG. 2017. Performance of five surface energy balance models for estimating daily evapotranspiration in high biomass sorghum, ISPRS Journal of Photogrammetry and Remote Sensing, 128; 192-203.

Wolff W, Francisco JP, Flumignan DL, Marin FR, Folegatti MV. 2022. Optimized algorithm for evapotranspiration retrieval via remote sensing, Agricultural Water Management, 262; 107390.

Yang Y, Shang S. 2013. A hybrid dual-source scheme and trapezoid framework–based evapotranspiration model (HTEM) using satellite images: Algorithm and model test, Journal of Geophysical Research: Atmospheres, 118; 2284-2300.

Yang Y, Shang S, Jiang L. 2012. Remote sensing temporal and spatial patterns of evapotranspiration and the responses to water management in a large irrigation district of North China, Agricultural and Forest Meteorology, 164; 112-122.

Zhou J, Zhang X, Zhan W, Zhang H. 2014. Land surface temperature retrieval from MODIS data by integrating regression models and the genetic algorithm in an arid region, Remote Sensing, 6; 5344-5367.

Zwart SJ, Bastiaanssen WG. 2007. SEBAL for detecting spatial variation of water productivity and scope for improvement in eight irrigated wheat systems, Agricultural Water Management, 89; 287-296.